

## High-intensity ion beams with submillisecond duration for synergistic of ion implantation and energy impact on the surface

*A.I. Ryabchikov, D.O. Sivin\*, S.V. Dektyarev, D.O. Vakhrushev*

*National Research Tomsk Polytechnic University, Tomsk, Russia*

*\*sivin@tpu.ru*

**Abstract.** The development of methods to modify materials based on the synergistic high-intensity implantation and simultaneous energy impact on the ion-doped layer involves using the pulsed and repetitively-pulsed beams of metal and gas ion beams with micro-submillisecond duration with high pulsed power density. The paper presents the results of experimental studies on the formation of pulsed and repetitively-pulsed high-intensity beams of titanium ions with a pulse duration from 150 to 500  $\mu$ s. The plasma flow was generated by a vacuum arc discharge. To obtain ion beams with a power density in the range from several tens to several hundreds of kilowatts per square centimeter, ballistic focusing of ions was used using an extracting grid electrode in the form of a part of a sphere. The features of the forming the high-power repetitively-pulsed beams of titanium ions were studied using both the ion source “Rainbow 5”. Data are presented on the influence of the ion beam space charge neutralization processes at current densities from fractions to several amperes per square centimeter on the efficiency of the ion beam’s transport and focusing at accelerating voltages from 10 to 30 kV.

**Keywords:** high-intensity ion beam, high-power density titanium ion beam, vacuum-arc plasma.

### 1. Introduction

Beams of charged particles and plasma flows are growing in use to modify the properties of various materials and coatings [1]. Pulsed energy impact on the solid surface has a special place in the technologies of ion-plasma processing of materials. Beams of electrons [2], ions [3], laser radiation [4], nano-, of microsecond duration with high power density provide modification of various metals and alloys due to extremely high rates of heating and subsequent cooling of surface layers at depths from a few to several tens of micrometers. In this case, the main process of modifying the microstructure and properties of materials is due to the superfast hardening effect without changing the elemental composition of the substance. An alternative method of beam modification of materials is based on ion implantation [5, 6]. Studying the features and regularities for modifying metals and alloys’ properties during customary ion implantation has shown the limited possibility of its practical application. The main limitation is associated with a small projective range of ions and, accordingly, with an insignificant ion-doped layer thickness.

New high-intensity implantation methods using low-energy high-power density ion beams have been developed in recent years. These methods have demonstrated the possibility of materials’ ion doping at depths of tens of micrometers at ion irradiation fluences of  $10^{19}$ – $10^{21}$  ion/cm<sup>2</sup> [7]. Good prospects for practical application were shown by high-intensity nitrogen ion implantation into stainless steel, AISI 5135 and AISI 420 steel [8, 9], when at implantation temperatures not exceeding 450–500 °C, modified layers with a thickness of tens and hundreds of micrometers were formed within an hour. It can be assumed that similar results can also be obtained in cases of low-energy high-intensity ion implantation with small atomic sizes. The advantages of the low-energy high-intensity ion implantation (LEHI3) method, providing deep ion doping of materials, are leveled out in a number of promising applications by heating the entire sample to high temperatures, at which degradation of the material microstructure is observed.

A new method described in [10] is aimed at solving the problem of maintaining the advantages of high-intensity implantation with simultaneous elimination of high-temperature degradation of the irradiated target microstructure. The essence of the method lies in the use for high-intensity implantation of ion beams with micro- or submillisecond duration with a power density from tens to several hundreds of kilowatts per square centimeter. Repetitively-pulsed implantation using such

ion beams can provide pulsed heating of a local region near the surface, followed by rapid heat transfer into the target material. Thus, a high temperature is achieved in the ion-doped layer and, simultaneously, the presence of a high temperature in the entire volume of the irradiated material is excluded. High temperature and high ion current density contribute to radiation-enhanced diffusion of implanted atoms, providing material ion doping at depths significantly exceeding the projective ion range. The effect of high-speed cooling of the surface layer due to the rapid heat transfer into the target material will improve the ion-doped layer microstructure. High ion current density, significant pulse duration, and a frequency regime of pulse formation can provide a high rate of ion irradiation fluence, which is necessary for deep ion doping of materials.

This article focuses on experimental study of the possibility and regularities of formation of repetitively-pulsed titanium ion beams with submillisecond duration with a power density of up to one hundred kilowatts per square centimeter.

## 2. Experimental setup and procedure of the experiment

Experimental studies were carried out using a complex installation for ion-beam and ion-plasma processing of materials. The pulsed and repetitively-pulsed titanium ion beams were formed using a modified source of ions and plasma “Rainbow 5”. The power supply system of the pulse transformer was upgraded in such a way as to form ion beams of various durations from 50 to 500  $\mu$ s. The plasma flow was formed by a continuous vacuum-arc discharge with an arc current of 120 and 160 A. The “solar eclipse” system was used instead of a louver-type plasma filter to clean plasma from the microdroplet fraction.

To form an ion beam with a high pulsed power density, a focusing system was used, which is a grid electrode in the form of a part of a sphere with a radius of 120 mm with an equipotential space for ion beam transport and focusing. Three grid electrodes with different cell sizes were used in the experiments: 0.5×0.5, 1×1, and 2.4×2.4 mm<sup>2</sup>. A disk electrode preventing the direct passage of macroparticles from the cathode’s working surface into the beam focusing region was installed at the focusing electrode center. The ions were extracted from the free boundary of the metal plasma generated by an arc discharge at anode bias potentials in the range from 9 to 30 kV.

During the experiments, the accelerating voltage, the current to the grid electrode, the ion beam current, and the total current of the voltage pulse generator were measured. To measure the ion current density distribution over the focused ion beam’s cross-section, six collectors with an area of 2×2 mm<sup>2</sup> were used. In the process of research, the pulsed voltage amplitude, the pulse duration, and the arc discharge current were changed. The beam ion current pulse had a significant high-frequency modulation. This complicated the estimation of the actual current amplitude and its density, and, as a consequence, the achievable power density in the ion beam. In this regard, to increase the accuracy of the current amplitude measurement, the mathematical smoothing was used. In some cases, averaging of current and voltage pulses over 15–25 oscillograms was used using the mathematical apparatus of the oscilloscope LeCroy “Waverunner 6050A”.

## 3. Studying the high-power density titanium ion beam formation

Initially, the experiments were carried out with a grid electrode with a radius of 120 mm and a cell size of 0.5×0.5 mm<sup>2</sup> at a continuous arc discharge current of 160 A. Single current pulse oscillograms demonstrate significant amplitude modulation during the entire pulse duration, Fig.1. This modulation is due both to the regularities of ion emission from the cathode spot of a vacuum-arc discharge and to the features of the high-intensity ion beam formation and transport.

Fig.2 shows typical oscillograms of the voltage pulse, the total current of the high-voltage transformer, and the ion current density in the focal region along the beam axis, averaged over 15 pulses for an accelerating voltage of about 20 kV. On averaged oscillograms, significant

modulation decreases many times, which makes it possible to determine the amplitude of the pulses sufficiently.

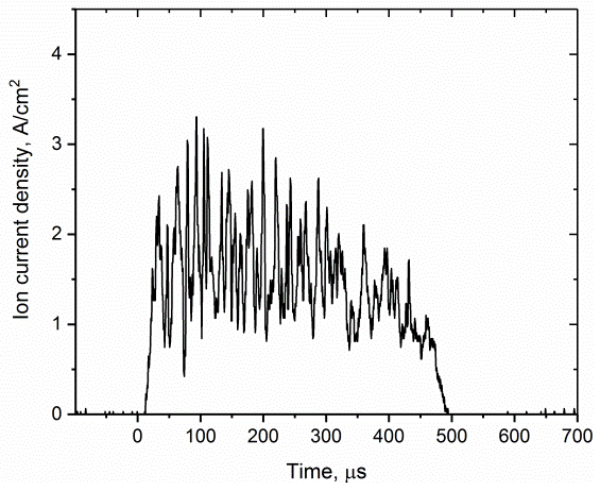


Fig.1. Single current pulse oscillogram obtained at an accelerating voltage amplitude of 25 kV.

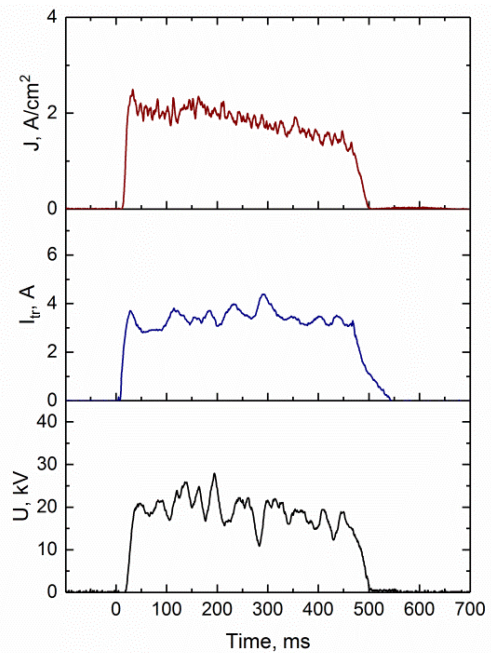


Fig.2. Oscillograms of the ion current density, accelerating voltage pulse, and total current of a high-voltage transformer, averaged over 15 pulses at an accelerating voltage amplitude of 20 kV.

Fig.3 shows the results of studying the influence of the accelerating voltage on the ion current density distribution over the beam cross-section. At an anode potential amplitude and, accordingly, plasma potential amplitude of 9 kV, the maximum ion current density of about  $2.75 \text{ A/cm}^2$  is reached.

The current density distribution over the cross-section is very narrow. A further increase in voltage to 16 kV leads to an increase in the maximum current density to  $3.25 \text{ A/cm}^2$ . In this case, a slight broadening of the current density distribution over the beam cross-section is observed. It is typical, that with further increase in voltage to 22 and 27 kV, the maximum current amplitude at the beam's center noticeably decreases to about  $2 \text{ A/cm}^2$ , and the beam width at half-height increases almost three times with the beam half-width at 9 kV. This behavior of the current density distribution can be associated with the ion beam charge neutralization in the drift space.

Initially, during the extraction of ions and their injection into the drift space, the beam charge is effectively neutralized due to the vacuum-arc plasma previously injected into the drift space. The neutralization time is determined by leaving of plasma ions from the beam. As shown by the results of numerical simulation, at low-energy high-intensity metal ion beam formation [11], this time does not exceed several microseconds. At the first stage, the ion density in the beam at the input to the drift space is almost an order of magnitude lower than the electron density in the plasma. This ensures a good degree of the ion beam charge neutralization both near the grid electrode and at a considerable distance in the drift space when it is focused with a proportional increase in the ion density. However, after sheath layer formation near the grid electrode, where ions are accelerated, the plasma flow, ensuring the supply of electrons to the drift space, stops. The production of electrons in the case of forming long pulses is possible due to ion-electron emission from structural elements of the beam formation system, as well as due to the plasma formation owing to residual

atmosphere atom ionization by ions. On the other hand, although the beam focusing and transport system in the initial state is an equipotential space, the presence of a grid electrode creates the condition for electrons to leave into the accelerating gap. The electric field of the accelerating gap penetrates into the drift space through the grid cells and performs the extraction of electrons, thereby worsening the beam space charge neutralization. An increase in the accelerating voltage amplitude should be accompanied by an intensification of the leaving of electrons from the drift space. It can also be assumed that the dynamically changing electric fields of the beam in the drift space will heat up the plasma electrons, facilitating their leaving from the ion beam. As a result, the ion beam transport and focusing will be affected by the balance of produced electrons and electrons leaving the drift space.

Studying the influence of the accelerating voltage pulse duration at an amplitude of 22 kV on the maximum ion density did not reveal significant features. Fig. 4 shows single oscillograms of current pulses with durations from 150 to 500  $\mu\text{s}$ . It can be noted that an increase in the pulse duration is accompanied by a gradual decrease in the current amplitude, which is presumably associated with a gradual deterioration in the conditions for the beam space charge neutralization and defocusing.

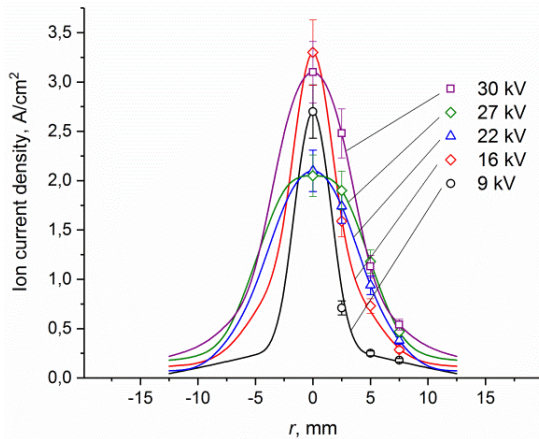


Fig.3. Distribution of the ion current density over the beam cross section for a formation system with a 120 mm grid electrode with a cell size of  $0.5 \times 0.5 \text{ mm}^2$  at a continuous arc discharge current of 160 A.

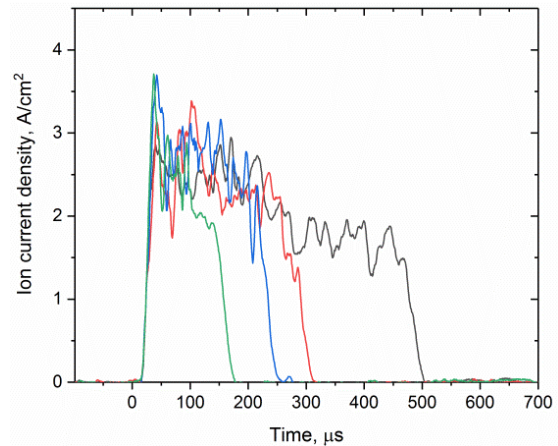


Fig.4. Single oscillograms of current pulses with durations from 150 to 500  $\mu\text{s}$  at an accelerating voltage amplitude of 22 kV.

The use of a grid electrode with a radius of 120 mm and a cell size of  $1 \times 1 \text{ mm}^2$  influenced the regularities of titanium ion beam transport and focusing. At an accelerating voltage of about 16 kV, the total transformer current approached 3 A. Oscillograms, showing the change in current densities on two collectors located at a distance of 2.5 mm from each other, show that the current density on them remained approximately the same amplitude with its slight modulation during the pulse (Fig.5a). Increasing the accelerating voltage to 25 kV is accompanied by an increase in modulation, as shown in Fig.5b. It can be noted that there is a tendency for the current density to decrease on the central collector. A further increase in the accelerating voltage to 30 kV led to a significant current density distribution over the beam cross-section. As can be seen from Fig.5b, the current density on the central collector has dramatically decreased. A significant decrease in the current density also takes place on the second collector. The ion beam modulation becomes essential. Such dynamics of changes in the ion current density distribution over the beam cross-section with an increase in the accelerating voltage can be explained by the deterioration in the space charge neutralization due to the increasing leaving of electrons and the gradual ion beam defocusing.

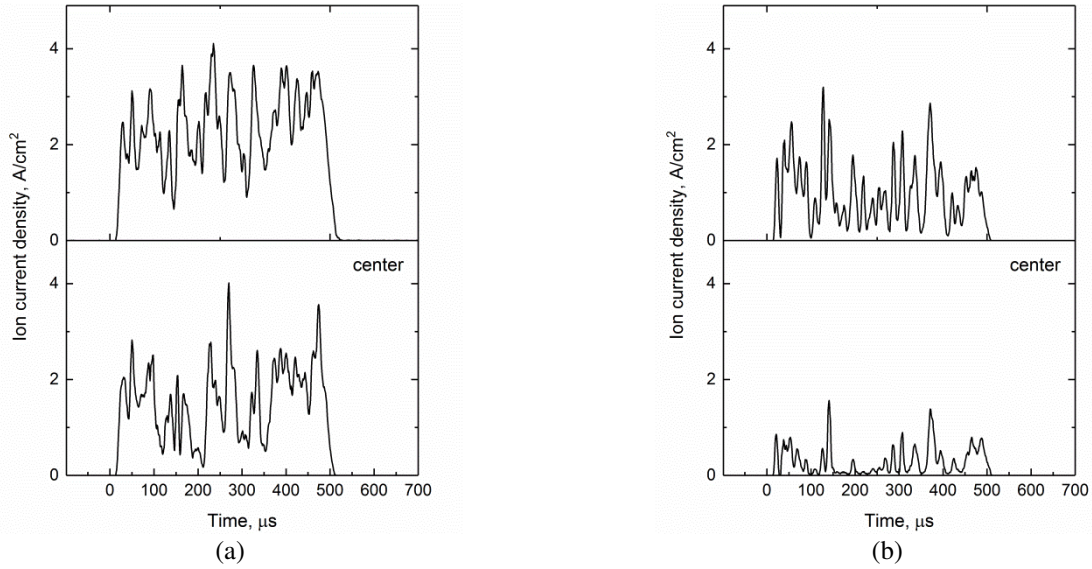


Fig.5. Oscillograms of the ion current density on collectors at the center of the beam at an accelerating voltage amplitude of 16 (a) and 25 kV (b).

A similar regularity in the high-intensity ion beam formation was observed with a grid electrode with a radius of 65 mm and a cell size of  $1.4 \times 1.4 \text{ mm}^2$ . At an accelerating voltage of 5 kV, the shapes of the current pulses on the collectors showed a maximum current at the center with an amplitude of up to  $0.7 \text{ A/cm}^2$ . With an increase in the accelerating voltage amplitude to 25 kV, the ion current density decreased almost to zero, and on the second and third collectors from the beam axis, the oscillograms showed a current density amplitude of up to  $0.25 \text{ A/cm}^2$  with a periodic modulation over the entire duration to zero.

Using a grid electrode with a radius of 120 mm and a cell size of  $2.4 \times 2.4 \text{ mm}^2$  showed a dramatic deterioration in the conditions for the high-intensity titanium ion beam formation. Fig.6 shows the oscillograms of the accelerating voltage pulse and the pulse transformer current and the ion current density on the central collector. Although the ion current density was  $1.5 \text{ A/cm}^2$ , it should be noted that the beam generation conditions are far from optimal.

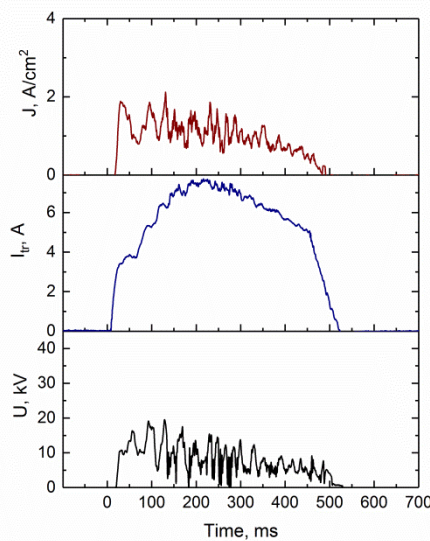


Fig.6. Oscillograms of the ion current density, accelerating voltage pulse, and total current of a high-voltage transformer for a formation system with a 120 mm grid electrode with a cell size of  $2.4 \times 2.4 \text{ mm}^2$ .

The transformer current oscillogram shows that the power supply was operating in overcurrent regime. The voltage oscillogram also indicates a significant decrease in amplitude compared to the normal operation regime of the pulse power supply. In conventional regime, the voltage amplitude should have been about 30 kV. As can be seen from Fig. 6 in this regime, the voltage amplitude does not exceed 12 kV with significant modulation during the entire pulse duration. Obviously, a grid electrode with a cell size of 2.4×2.4 mm<sup>2</sup> does not ensure the conservation of electrons that compensate for the space charge in the beam drift space. Plasma electrons and secondary electrons leave almost unhindered through the grid cells, increasing the total current amplitude in the accelerating gap, which leads to a catastrophic deterioration in the operating conditions of the pulsed voltage generator. It should be noted that a similar problem also occurred in conventional ion sources, where additional electrodes with a negative potential with an amplitude of up to several kilovolts were used to cut off the electron flow from the beam drift space to the accelerating gap.

#### 4. Conclusion

It has been shown for the first time that the use of a continuous vacuum-arc discharge with a current of up to 160 A in combination with an axially symmetric focusing system in the form of a grid electrode with a radius of 120 mm at accelerating voltages of up to 30 kV makes it possible to form a titanium ion beam with a power density approaching 100 kW/cm<sup>2</sup> with submillisecond pulse duration. The possibility of generating high-power density pulsed ion beams with duration from 150 to 500 μs is shown. Experiments with grid electrodes showed that with an increase in the grid cell size from 0.5×0.5 to 2.4×2.4 mm<sup>2</sup>, the conditions for the ion beam focusing and transport change significantly. An increase in the grid cell size is accompanied by an intensification of selecting electrons from the beam drift space to the accelerating gap and deterioration in the conditions for beam space charge neutralization. In the case of using a grid electrode with a grid cell size of more than 1.4×1.4 mm<sup>2</sup>, an increase in the accelerating voltage is accompanied by a decrease in the current density along the beam axis to almost zero, which indicates that the beam becomes hollow.

#### Aacknowledgements

This work was financially supported by the Russian Science Foundation (project No. 22-19-00051, <https://rscf.ru/project/22-19-00051/>).

#### 5. References

- [1] Williams J.S., Poate J.M., *Ion Implantation and Beam Processing*, (Orlando: Academic, 1984).
- [2] Shulov V.A., Paikin A.G., Teryaev D.A., Bytsenko O.A., Engel'ko V.I., and Tkachenko K.I., *Inorganic Mater., Appl. Res.*, **4**(3), 189, 2013; doi: 10.1134/S2075113313030118
- [3] Rej D.J., Davis H.A. and Olson J.C., *J. Vac. Sci. Technol. A, Vac., Surf., Films*, **15**(3), 1089, 1997; doi: 10.1116/1.580435
- [4] Poate J.M., Foti G., Jacobson D.C. *Surface Modification and Alloying by Laser, Ion, and Electron Beams*. (Berlin: Springer, 2013).
- [5] Ryabchikov A.I., Nasyrov R.A., *Rev. Sci. Instrum.*, **63**(4), 2428, 1992; doi: 10.1063/1.1142900
- [6] Anders A., *Handbook of Plasma Immersion Implantation and Deposition*. (New York: Wiley, 2000).
- [7] Ryabchikov A.I., *Surf. Coat. Technol.*, **388**, 125561, 2020; doi: 10.1016/j.surfcoat.2020.125561
- [8] Ryabchikov A., Sivin D., Ananin P., Lopatin I., Korneva O., Shevelev A., *Surf. Coat. Technol.*, **355**, 129, 2018; doi: 10.1016/j.surfcoat.2018.02.110

- [9] Ryabchikov A.I., Sivin D.O., Korneva O.S., Bozhko I.A., Ivanova A.I., *Surf. Coat. Technol.*, **388**, 125557, 2020; doi: 10.1016/j.surfcoat.2020.125557
- [10] Ryabchikov A.I., *IEEE Trans. Plasma Sci.*, **49**(9), 2529, 2021; doi: 10.1109/TPS.2021.3073942
- [11] Koval T.V., Ryabchikov A.I., Tran My Kim An, Shevelev A.E., Sivin D.O., Ivanova A.I., Paltsev D.M., *J. Phys.: Conf. Ser.*, **1115**, 032007, 2018; doi:10.1088/1742-6596/1115/3/032007